QIRT 10
http://dx.doi.org/10.21611/qirt.2010.130
10th International Conference on Quantitative InfraRed Thermography
July 27-30, 2010, Québec (Canada)

Application of the Source Distribution Image (SDI) procedure for porosity detection in honeycomb structures

by M. Susa*, X. Maldague** and I. Boras*

*Faculty of Mechanical Engineering and Naval Architecture, I. Lucica 5, 10000 Zagreb, Croatia, mirela.susa@fsb.hr
** ECE Dept., Université Laval, Québec (Quebec), Canada G1V 0A6, xavier.maldague@gel.ulaval.ca

Abstract

The article presents the results of Pulse Thermography experiment applied on a complex multi-layer honeycomb-based sample. The sample was a part of the aircraft and it was replaced because of the appearance of porosity in the adhesive layer of the assembly. The exact location, shape and level of porosity were not known. Non-uniform heating of the sample was limiting factor for the quality of the analysis results. The difficulty in determining the area where the porosity appeared was overcome using the Source Distribution Image procedure which takes into account the distribution of the heating non-uniformity when thermal image of the sample is analysed. The results obtained matched well the results obtained using ultrasonic inspection.

1. Introduction

Complex multi-layer composite structures are commonly used in aircraft construction for years now. They are tested using different non-destructive testing methods both during their production as well as in operation. Typical defects which occur in such multilayer structures include delaminations within several layers of the same material [1], disbonds which are the result of locally missing adhesive layer [2], porosity which occurs in the adhesive layer either during the production stage or during the in service period of the aircraft part [3], water inclusions in honeycomb structure [4] and other. All of these defects degrade significantly mechanical properties of the material and if they are important, can compromise the normal functioning of the entire aircraft.

2. Tested sample and experiment description

The sample analyzed was a real out-of-use aircraft part, which was known to have the porosity present in the adhesive layer, used for assembling the CFRP skin to the honeycomb aluminum core. Left-hand side of the Figure 1 shows the part of the sample inspected using PT, corresponding to the part 4 in the right-hand side of the same figure, which presents the whole aircraft part which was cut out for the overall inspection.

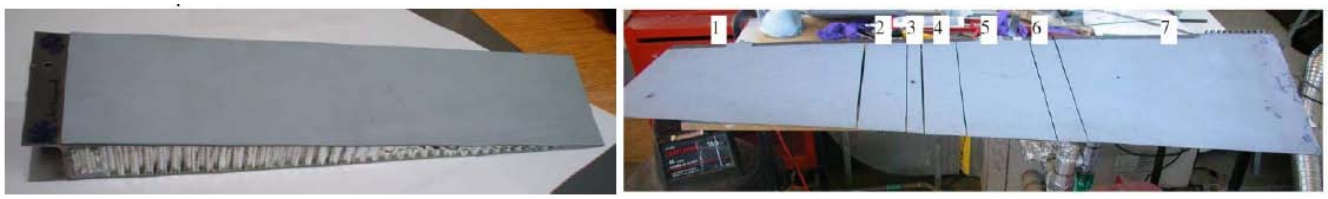

Fig. 1. *Left: Tested sample; Right: Whole aircraft part, tested sample is marked with number four*

In addition, in Figure 2 a microscopic structure of the defect type can be seen as obtained for the cross-sectional cut over the tested sample [3]. It can be seen that porosity is a defect which occurs at the contact between the CFRP skin and the adhesive layer in form of the small air bubbles which are responsible for the reduced mechanical properties of the assembled multilayer structure. Although the depth at which the defect appears can be well predicted from the material structure itself, the exact area affected by porosity needs to be assessed adequately.

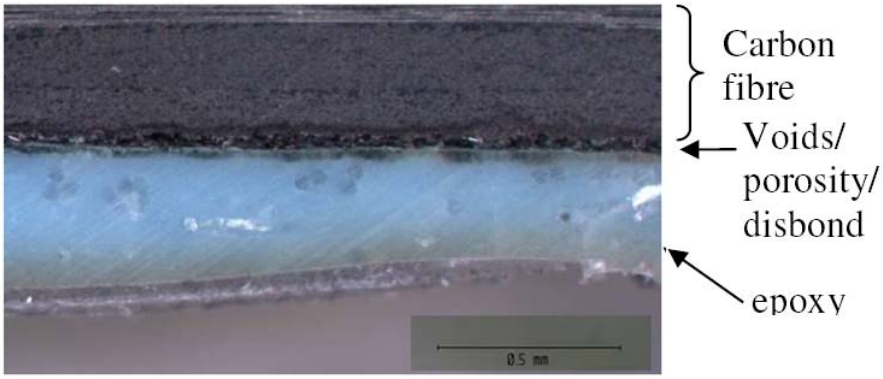

Fig. 2. *Cross-section of the tested sample. Microscopic structure of the porosity is visible.*

In our case, the Pulse thermography testing procedure was applied to the sample. The sample was tested in the reflection mode. In addition, it was tested in two parts, so that a better spatial resolution of the obtained images is achieved. Since it was not known in which of the two sides of the sample the porosity was present, the sample was also tested from both front and rear side. All the experiments were done one after another, so that the experimental conditions remain very similar. However, a sufficient time was left between two experiments in order to permit the sample to come back completely into the thermal equilibrium with the environment. Thermograms were recorded with frequency of 42.43 frames per second, permitting the recording a total of about 40 s of the experiment duration. The integration time was 1.9 ms. Image sequence was stored on the computer for later processing purposes.

3. Processing technique description

Immediately after the experimental results were acquired, their analysis proved that it was extremely difficult to determine where exactly a defective region was from the obtained thermograms, particularly due to the fact that the defect was expected to have an irregular shape which was not known a priori. In addition, it was not known from the start whether the sample was completely affected by the porosity, or there were sane regions still left in some sample parts. The non-uniform heating present in the experiment added to the difficulties in the defect detection as its shape was potentially hiding the defective regions contours. The effects of the nonuniform heating present in the experiment can be clearly seen on Figure 3. which represents the reconstructed Source Distribution Image (SDI).

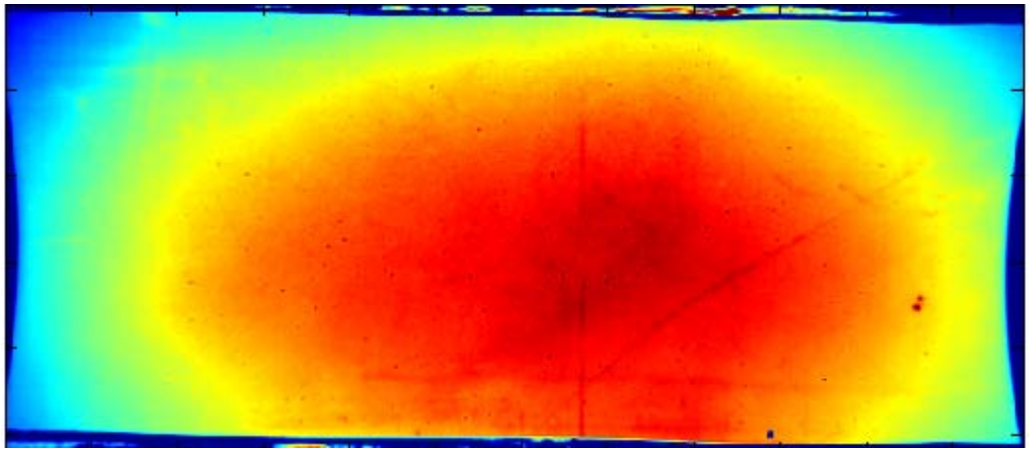

Fig. 3 *The reconstructed SDI showing showing the effects of the non-uniform heating*

The Source Distribution Image technique previously proposed by the authors [5] was used to assess the effects of the non-uniform heating. The technique consists of creation of the Source Distribution Image from the 2 or 3 first thermograms right after the heat pulse was applied to the sample. The SDI is created by finding the average pixel value of all the thermograms included on a pixel by pixel basis. The SDI is then used for the creation of the iso-value contours which are

http://dx.doi.org/10.21611/qirt.2010.130

the indicators of the spatial distribution of the heat source power. The span between two iso-values is defined small enough to enable the identification of regions within which the source power was relatively uniform.

4. Results and discussion

The outcome of this image treatment operation permitted, the defect detection itself, as it was not until the proposed SDI procedure was applied that the detection of the sane and defective regions was enabled. To explain how this was done, reference to the Figure 4 is needed. The figure shows a thermogram taken at 1.6 s after the heat pulse application. In the thermal image different levels of iso-temperatures were marked with black curves. The red curve represents one chosen iso-level line of the reconstructed SDI shown on Figure 3.

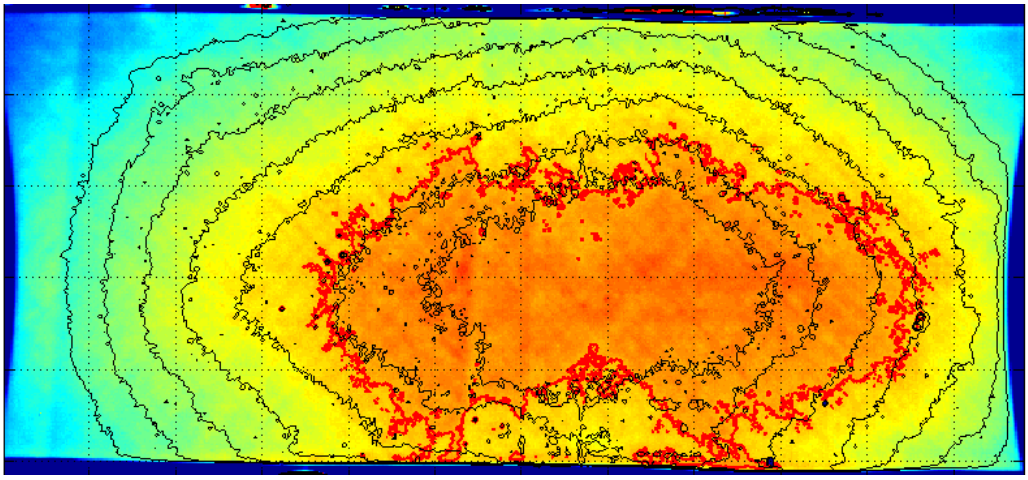

Fig. 4 *Superposition of a single isothermal level (red line) on a single thermogram taken from the sequence with different SDI level contours (black lines)*

The first thing which should be noticed when one looks at the Figure 4 is that the contours of the same color in the thermogram image corresponding to the same surface temperatures do not coincide in their shape with the shape of the iso-lines of the SDI. Yet it is exactly that shape that the contours of the iso-temperatures should be following (in the form of the quasi concentric irregular shapes) as the thermograms are acquired over the time, recording the evolution of the heat surface temperature. Thus, it was concluded that by choosing two points corresponding to the same iso-zone of the SDI and having significantly different thermal values, thermal contrast of a defect would be obtained (or in the extreme case where no sane region existed, the temperature difference between the two different degree porosity regions would be available through the obtained thermal contrast).

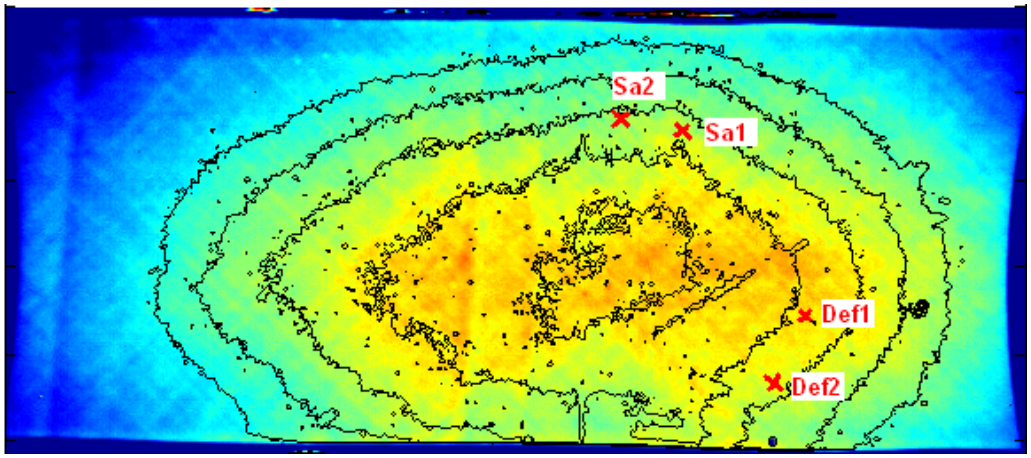

Fig. 5 *Application of the SDI range levels on the thermogram taken at 1.2 s after heat pulse permits to distinguish the defective regions*

http://dx.doi.org/10.21611/qirt.2010.130
10th International Conference on Quantitative InfraRed Thermography

Figure 5 shows the application of the defined spans of the iso-values obtained from the SDI segmentation onto the experimentally obtained thermogram about 1.2 s after the heat pulse, the time for which, as it was determined *a posteriori*, one of the defects showed its maximum thermal contrast value. Two chosen pairs of defective and sound regions are marked with red crosses in Figure 5.

All four selected points are located between two SDI iso-lines. However defect 1 (Def1) and its corresponding sane region 1 (Sa1) were both selected closer to the first SDI iso-line (corresponding to the higher level of the source power applied) whereas the defect 2 (Def2) and its corresponding sane region 2 (Sa2) were selected closer to the second SDI iso-line (corresponding to the lower level of the source power applied). Figure 6 shows the time evolution of the surface temperature contrast obtained for the two sets of defective-sane points.

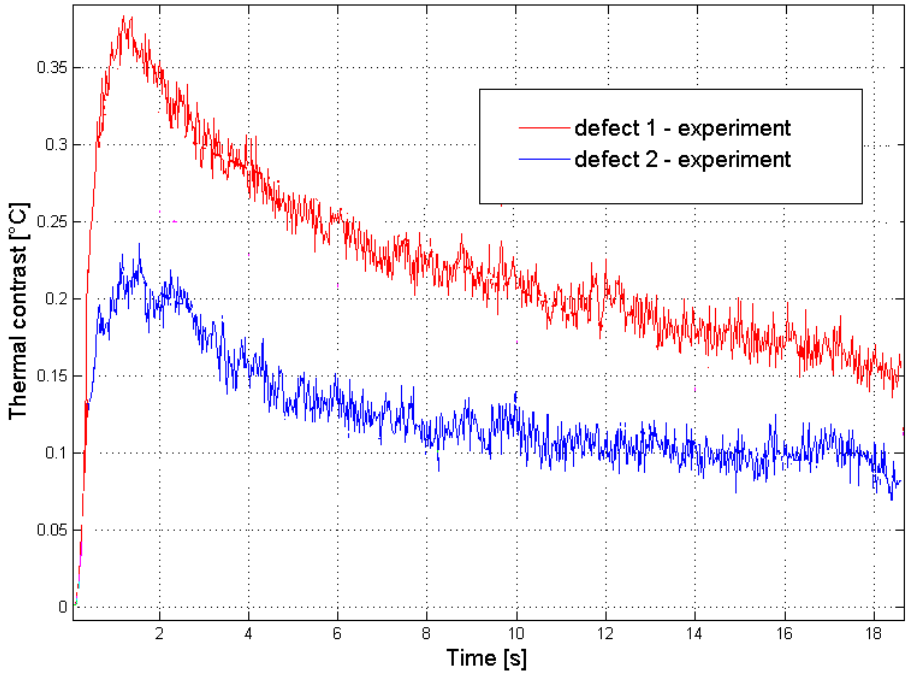

Fig. 6 *Time evolution of the surface temperature contrast for two defects*

Even though the exact geometry and porosity characteristics of the sample were not known, the shape of the thermal contrast curve exhibiting the expected bell shaped curve characteristic for the thermal contrast of defect, is a good indicator of the presence of the defect within a sample. However, unless it is *a priori* known which region is in fact entirely porosity-free, or unless a valid numerical results could be used as reference, it is not possible to claim with certainty whether the thermal contrast obtained is due to the different thermal behaviour of the porosity- affected and porosity-free region or to the different thermal behaviour of two different degrees of porosity present in the sample.

The ultrasound echo-pulse c-scan of the tested honeycomb part can be seen in Figure 7. The right-hand double-framed section of the ultrasound image corresponds to the full length of the thermogram depicted in Figure 4.with blue ellipse indicating the region within which the defective and sane regions were chosen for thermal contrast evolution curves in Figure 6 to be constructed. The irregular black curves were added semi-automatically indicating the contours of the different porosity regions (sane and defective area). The correspondence of the defective region shapes and surfaces obtained by the two methods (black curve in the ultrasound image and red curve obtained as an iso-line in the SDI image are noticed, despite the difference in the scales of the two images. By choosing the sane regions in the green colourer areas and defective regions from the reddish coloured regions in Figure 7 taking at the same time into account the non-uniform heating effects by applying the SDI technique for appropriate corresponding sane and defective regions selection, it is expected that better quality thermal contrast evolution curves are obtained.

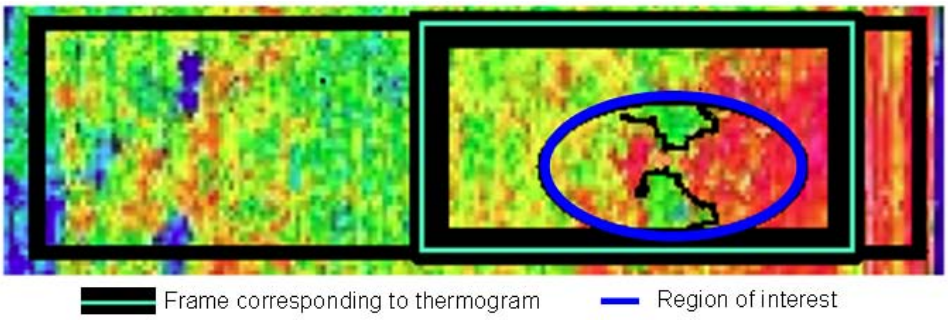

Fig. 7 *The ultrasound echo-pulse c-scan of the tested honeycomb part*

5. Conclusion

The comparative result presented in this paper give confidence in the usefulness which SDI might have for the detection of the irregular-shape defects tested in the non-uniform heating conditions which cannot be eliminated in the experimental procedure. Independently performed ultrasound non-destructive testing procedure revealed significant correspondence between the results of the two NDT methods indicating that proposed SDI technique brings a definite value add to the analysis of the pulse thermography experimental results. What is more, as previous publications already pointed out, the use of SDI technique improves the quality of the results obtained for thermal contract evolutions which are of high importance for further defect characterization procedures.

Presented results indicate that further investigation in this field could be promising, in particular given that porosity in aircraft construction materials is a common defect and that it is of highly irregular and unpredictable shape, which makes it difficult to be identified and evaluated. Further research activities in this field should be directed toward additional confirmation of the procedure through more comparative experimental results as well as through the development of the appropriate numerical models which would contribute to the evaluation of the porosity degrees.

REFERENCES

[1] Vavilov V., “Peculiarities of detecting teflon defect surrogates in CFRP by transient IR thermography”, Quantitative Infrared Thermography, Proceedings of QIRT, Vol.7, p.145-151, 2004.
[2] Ahrens R.O., “Fabrication of sandwich material, honeycomb core, carbon skins - fabrication procedures and process specification”, Boeing St. Louis, 1977 (revised 1999).
[3] Genest M., “F-18 Rudder Pull Tests”, Laboratory memorandum, Institute for Aerospace Research, Canada, 2007.
[4] Vavilov V.P. and Nesteruk D.A., “Detecting water in aviation honeycomb structures: the quantitative approach”, QIRT Journal, Vol.1, p.173-184, 2004.
[5] Susa M., Maldague X. And Boras I., “Improved method for absolute thermal contrast evaluation using Source Distribution Image (SDI)”, Infrared Physics and Technology, Vol. 53, p. 197-203, 2010.